it is possible to deduce for $x = 0$,

$$\sum_1^\infty \frac{1}{n^2+\omega^2} = \frac{\pi}{2\omega \tanh \omega\pi} - \frac{1}{2\omega^2}$$

and for $\omega = ia$, i.e., $\omega^2 = -a^2$,

$$\sum_1^\infty \frac{1}{n^2-a^2} = \frac{-\pi}{2a \tan a\pi} + \frac{1}{2a^2}$$

$$\sum_1^\infty \frac{(-1)^n \cos nx}{n^2-a^2} = \frac{-\pi \cos ax}{2a \sin a\pi} + \frac{1}{2a^2}$$

$$\sum_1^\infty \frac{(-1)^{m-1} m \sin mx}{m^2-A^2} = \frac{\pi}{2} \frac{\sin xA}{\sin \pi A}.$$

References

[1] A. F. Harvey, "Periodic and guiding structures at microwave frequencies," *IRE Trans. Microwave Theory Tech.*, pp. 30–61, Jan. 1960.

[2] G. H. Bryant, "Propagation in corrugated waveguides," *Proc. Inst. Elec. Eng.*, vol. 116, pp. 203–213, Feb. 1969.

[3] Y. Garault, "Hybrid EH guides waves: Their application to microwave separators of High Energy Particules," in *Advances in Microwaves*, vol. 5, L. Young, Ed. New York and London. Academic Press, 1970.

[4] A. J. Sangster and H. G. Donald, "An analysis of an abrupt transition from a uniform empty waveguide to a periodically loaded waveguide," *Int. J. Electron.*, vol. 55, no. 2, pp. 213–227, 1983.

[5] Y. Garault and J. P. Fenelon, "Détermination de la caractéristique de dispersion d'une cavité périodique ouverte à l'aide d'une cavité de longueur variable à un seul iris" ("Determination of the dispersion characteristic of an open periodic structure with the help of a variable length cavity with a single iris") *Comptes-rendus — Académie des Sciences Paris*, vol. 276, série B, pp. 409–412, Mar. 12, 1973.

[6] K. Kurokawa, "The expansions of electromagnetic fields in cavities," *IRE Trans. Microwave Theory Tech.*, vol. 6, pp. 178–187, Apr. 1958.

[7] J. Van Bladel, *Electromagnetic Fields*. New York. McGraw-Hill, 1964.

[8] Y. Garault and J. P. Fenelon, "Les ondes hybrides EH dans un guide en auge périodique." ("Hybrid EH waves in a trough waveguide with periodic corrugation") *Comptes-rendus — Academie des Sciences Paris*, vol. 267, série B, pp. 540–543, Sept. 9, 1968.

[9] R. M. Bevensee, Ed., *Electromagnetic Slow Waves Systems*. New York: Chapter III, pg. 63–91. Wiley, 1964, Ch. III, pp. 63–91.

[10] J. P. Fenelon, Thesis of "Doctorat d'Etat es Sciences" degree, Limoges University, Sept. 5, 1985.

[11] I. S. Gradshteyn and I. M. Ryzhik, *Tables of Integrals, Series and Products*. New York and London: Academic Press, 1965.

Design of New Hybrid-Ring Directional Coupler Using λ/8 or λ/6 Sections

Dong Il Kim and Gyu-Sik Yang

Abstract—**A method for designing 1.25λ-ring and 7λ/6-ring 3 dB directional couplers using fundamental λ/8 or λ/6 sections is proposed and their frequency characteristics are analyzed. Furthermore, experimental verification has been achieved in a microstrip network, confirming the validity of the design method for a microwave component with the basic λ/8 or λ/6 sections proposed in this paper.**

Manuscript received February 22, 1991; revised May 6, 1991. This work was supported by the Korea Science and Engineering Foundation.

The authors are with the Department of Electronics and Communications Engineering, Korea Maritime University, Youngdo-ku, Pusan 606-791, Korea.

IEEE Log Number 9102323.

I. Introduction

The hybrid-ring directional coupler was one of the first and remains one of the most fundamental junctions in the microwave and millimeter-wave frequency bands [1]–[6] where one-axis symmetry is involved. Important properties possessed by all directional couplers are 1) the output arms are isolated from each other and 2) the input arms are matched looking into any arm when the other arms are terminated by matched loads. Since the conventional, simple Y-junction power dividers do not possess these properties, directional couplers are preferable for certain applications, for example antenna array feed systems where the need for minimizing mutual coupling puts a premium on isolation between the output arms of the power dividers [2].

The two-dimensional structure of stripline facilitates construction of the feeding network and antenna elements, such as dipoles, on a single printed circuit board. At high frequencies, some applications make hybrid-ring couplers preferable to branch-line and parallel-line couplers; the former has an inherent 90° phase difference between the output ports. For an antenna array that is fed by an equiphase, symmetrical, corporate network, the hybrid-ring directional coupler has a definite advantage over the parallel-line and branch-line couplers because no phase-compensating element is necessary. The hybrid-ring coupler also has a broader bandwidth than the branch-line coupler [2], [4].

The hybrid-ring directional coupler is well known as a rat race ring which is used for a 3 dB directional coupler with the normalized admittance of $1/\sqrt{2}$ of the entire circumference of the ring [5]. In 1961 Pon proposed a hybrid-ring coupler having a power-split ratio that is proportional to the square of the admittance ratio of the two variable admittances in the ring [2]. In 1982, Kim and Naito developed a broad-band design method of improved hybrid-ring 3 dB directional couplers where the concept of a hypothetical port was adapted [5]. In 1986, Agrawal and Mikucki designed a hybrid-ring directional coupler with arbitrary power divisions by adapting Pon's method to Kim and Naito's concept of a hypothetical port [4]. However, all branch-line couplers, parallel-line couplers, and hybrid-ring couplers, including the rat-race ring, consist of a common fundamental $\lambda/4$ sections. In addition, most microwave components also use fundamental $\lambda/4$ lines.

In this paper, however, we propose a design method for 1.25λ-ring and 7λ/6-ring 3 dB directional couplers using $\lambda/8$ and $\lambda/6$ sections, respectively. In addition, the frequency characteristics of the couplings, together with the isolations, the return losses, and the phase differences between the output ports, are calculated.

II. Analysis and Design of λ/8- and λ/6-Section 3 dB Directional Couplers

The conventional hybrid-ring directional coupler has the configuration shown in Fig. 1 [2]. To increase the degree of freedom of the design, while maintaining symmetry, we can replace the characteristic admittance Y_1 of the $3\lambda/4$ section across the symmetrical axis AA' by Y_3 and replace the lengths $\lambda/4$ and $3\lambda/4$ of two sections across the symmetrical axis AA' by $\lambda/8$

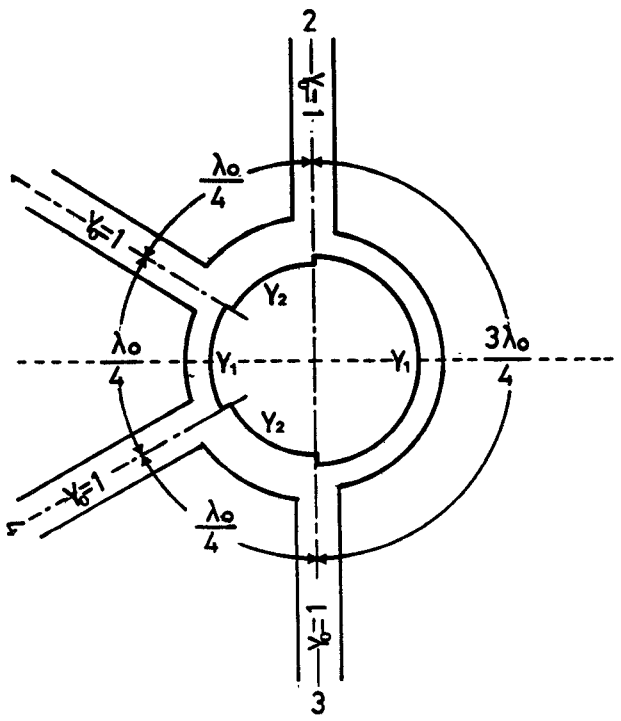

Fig. 1. Conventional hybrid-ring directional coupler.

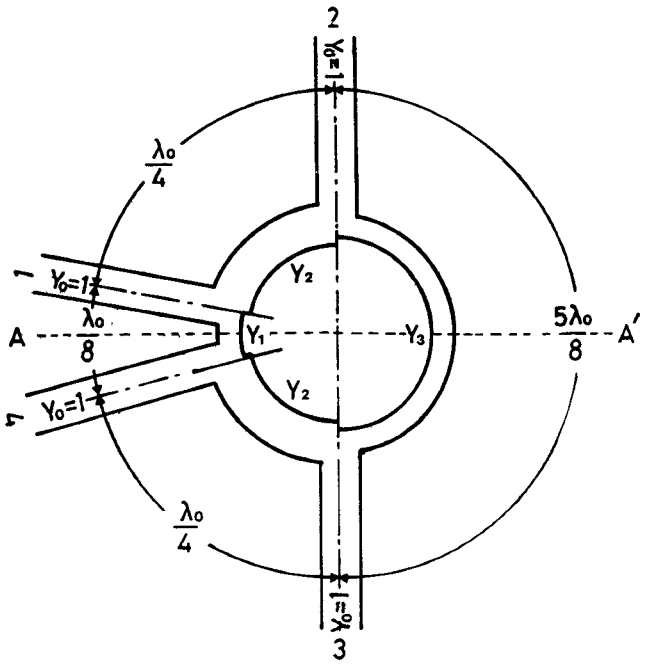

Fig. 2. Configuration of an 1.25 wavelength hybrid ring.

and $5\lambda/8$, respectively. Then, the whole circumference of the ring of the directional coupler becomes 1.25λ, as shown in Fig. 2. Similarly, the lengths $\lambda/4$, $\lambda/4$, and $3\lambda/4$ of the sections Y_1, Y_2, and Y_3 can be replaced by $\lambda/6$, $\lambda/6$, and $4\lambda/6$ as shown in Fig. 3, yielding the $7\lambda/6$-ring directional coupler.

To analyze the frequency response characteristics of the 1.25λ-ring and the $7\lambda/6$-ring couplers, we represent the equivalent circuits shown in Fig. 4. The values of y_1 and y_3 for the even- and odd-mode excitations can be obtained [7].

In general, the scattering matrix, $[S]$, representing the input–output relation for a reciprocal junction with one-axis

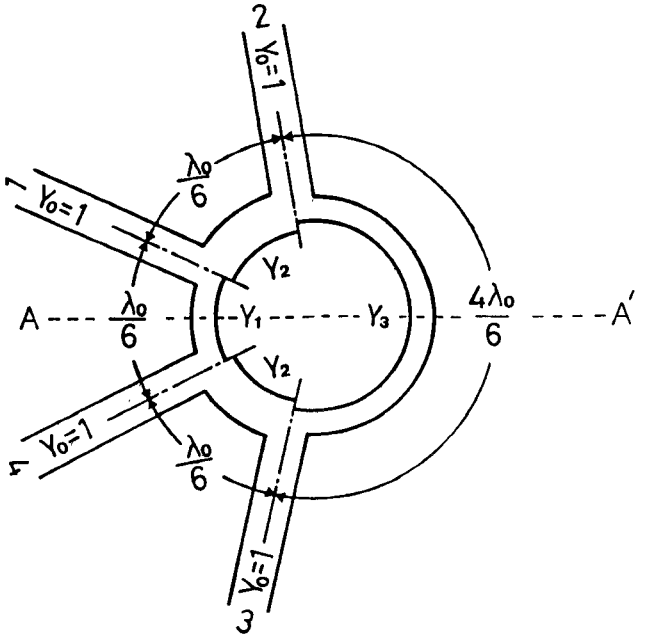

Fig. 3. Configuration of a 7/6 wavelength hybrid ring.

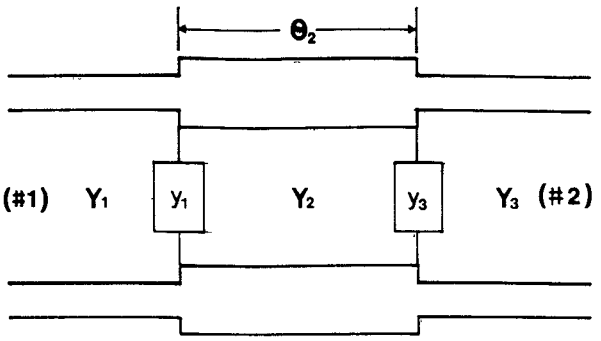

Fig. 4. Equivalent circuit for even- or odd-mode excitation.

symmetry, as shown in Figs. 1, 2, and 3, is represented by

$$[S]=\begin{bmatrix} S_{11} & S_{12} & S_{13} & S_{14} \\ S_{21} & S_{22} & S_{23} & S_{24} \\ S_{31} & S_{32} & S_{33} & S_{34} \\ S_{41} & S_{42} & S_{43} & S_{44} \end{bmatrix}=\begin{bmatrix} S_{11} & S_{12} & S_{13} & S_{14} \\ S_{12} & S_{22} & S_{23} & S_{13} \\ S_{13} & S_{23} & S_{22} & S_{12} \\ S_{14} & S_{13} & S_{12} & S_{11} \end{bmatrix}. \quad (1)$$

A. 1.25λ-Ring Directional Coupler

The scattering parameters of the 1.25λ-ring coupler are found by

$$S_{11}=\frac{j\left(1-Y_1^2-Y_2^2\right)}{2Y_1+j\left(1+Y_1^2+Y_2^2\right)}$$

$$S_{41}=\frac{2\sqrt{2}\,Y_1}{2Y_1+j\left(1+Y_1^2+Y_2^2\right)}$$

$$S_{21}=\frac{2Y_2}{2Y_1+j\left(1+Y_1^2+Y_2^2\right)}$$

$$S_{22}=S_{11}$$

$$S_{32}=-S_{41}$$

$$S_{12}=S_{21}$$

$$S_{41}=S_{31}=0. \quad (2)$$

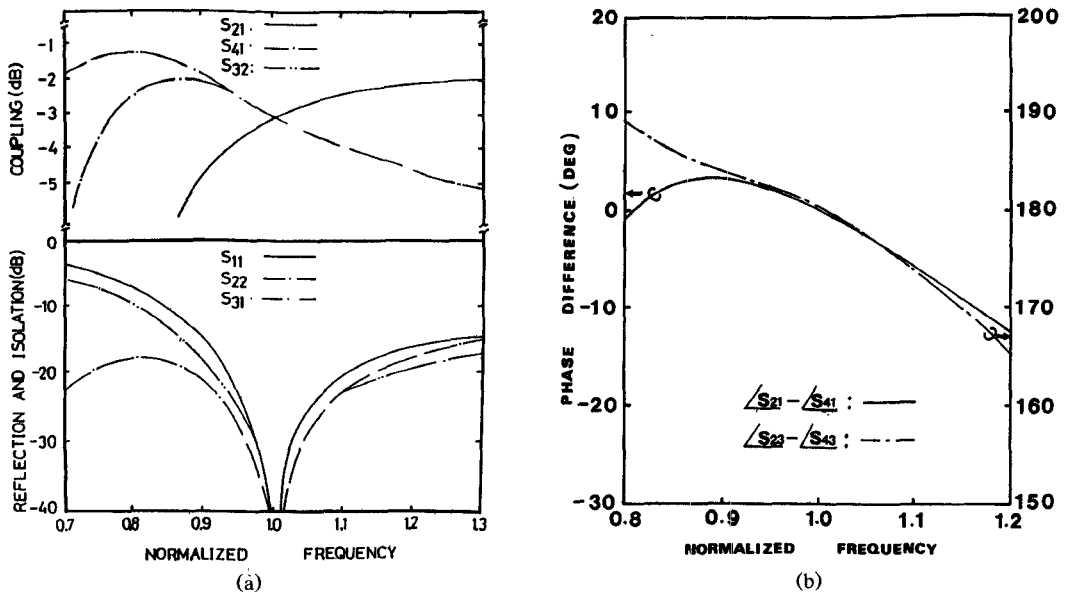

Fig. 5. Theoretical study with three functions: △ distribution, ◇ exponential, and ○ 1/SQRT, □ Experimental study. Period $H = 10$ mm.

From (2) we can see that two output arms are isolated from each other since $S_{31} = S_{42} = 0$. The condition that the input arm be perfectly matched requires that S_{11} and S_{22} in (2) be zero, from which we get

$$Y_1^2 + Y_2^2 = 1. \tag{3}$$

The condition for 3 dB output power division requires that $|S_{21}| = |S_{41}|$ and $|S_{12}| = |S_{32}|$ in (2), from which we get

$$Y_2 = \sqrt{2}\, Y_1. \tag{4}$$

Thus, the 1.25λ-ring 3 dB directional coupler can be designed by taking $Y_1 = 1/\sqrt{3}$ and $Y_2 = \sqrt{2/3}$, which can be seen from (3) and (4), and the output voltage ratio (couplings) between the output arms can be adjusted by varying Y_1 and Y_2.

B. 7λ/6-Ring Directional Coupler

Similarly, we obtained the scattering parameters as follows:

$$S_{11} = (1/2)\frac{j\{\sqrt{3} + (2\sqrt{3}/3)Y_1Y_2 - \sqrt{3}Y_2^2 - (\sqrt{3}Y_1^2\}}{Y_1 + Y_2 + j\{(\sqrt{3}/2) - (\sqrt{3}/3)Y_1Y_2 + (\sqrt{3}/2)Y_2^2 + (\sqrt{3}/2)Y_1^2\}}$$

$$S_{41} = (1/2)\frac{4Y_1}{Y_1 + Y_2 + j\{(\sqrt{3}/2) - (\sqrt{3}/3)Y_1Y_2 + (\sqrt{3}/2)Y_2^2 + (\sqrt{3}/2)Y_1^2\}}$$

$$S_{21} = (1/2)\frac{4Y_2}{Y_1 + Y_2 + j\{(\sqrt{3}/2) - (\sqrt{3}/3)Y_1Y_2 + (\sqrt{3}/2)Y_2^2 + (\sqrt{3}/2)Y_1^2\}}$$

$$S_{22} = S_{11} \qquad S_{32} = S_{41} \qquad S_{42} = 0 = S_{31}. \tag{5}$$

From (5) we can see that two output ports are isolated from each other since $S_{31} = S_{42} = 0$ at $f = f_0$.

The condition for 3 dB output power division requires that $|S_{21}| = |S_{41}|$ and $|S_{12}| = |S_{32}|$ in (5), respectively, from which we obtain

$$Y_1 = Y_2 = Y \tag{6}$$

and the condition that the input arm be perfectly matched requires that S_{11} and S_{22} in (5) be zero, from which we get

$$Y = \sqrt{3/4}. \tag{7}$$

Thus, it has been shown that the 7λ/6-ring 3 dB directional coupler can be designed by taking the normalized characteristic admittance Y as $\sqrt{3/4}$ on the whole circumference.

III. Theoretical Frequency Characteristics

Fig. 5(a) shows the theoretical frequency characteristics of coupling, reflection, and isolation for the 1.25λ-ring 3 dB directional coupler designed in Section II, while Fig. 5(b) shows the phase differences between outputs for the coupler. The characteristic admittance and the length of each section are represented in Table I.

Fig. 6(a) shows the theoretical frequency characteristics of couplings, reflection, and isolation for the 7λ/6-ring 3 dB direc-

TABLE I
DESIGNED 7λ/6-RING HYBRID COUPLER

Section	Y_1	Y_2	Y_3
Normalized characteristic admittance	$\sqrt{3/4}$	$\sqrt{3/4}$	$\sqrt{3/4}$
Length of each section	$\lambda/6$	$\lambda/6$	$2\lambda/3$

TABLE II
DESIGNED 1.25λ-RING HYBRID COUPLER

Section	Y_1	Y_2	Y_3
Normalized characteristic admittance	$1/\sqrt{3}$	$\sqrt{2/3}$	$1/\sqrt{3}$
Length of each section	$\lambda/8$	$\lambda/4$	$5\lambda/8$

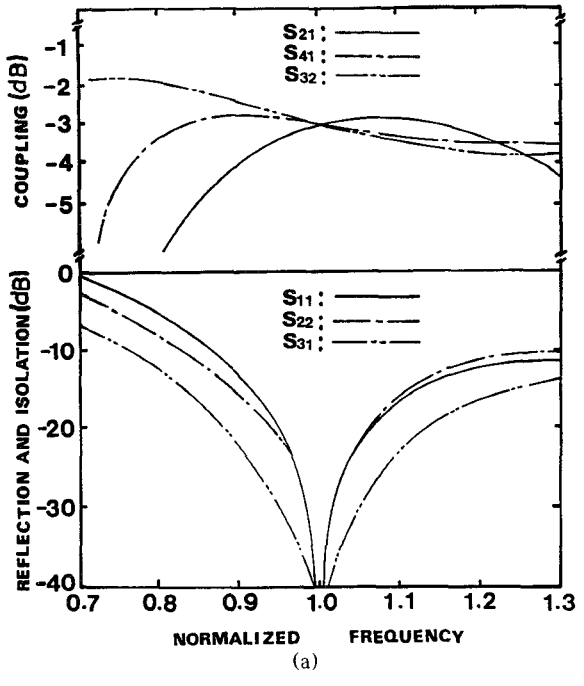

(a)

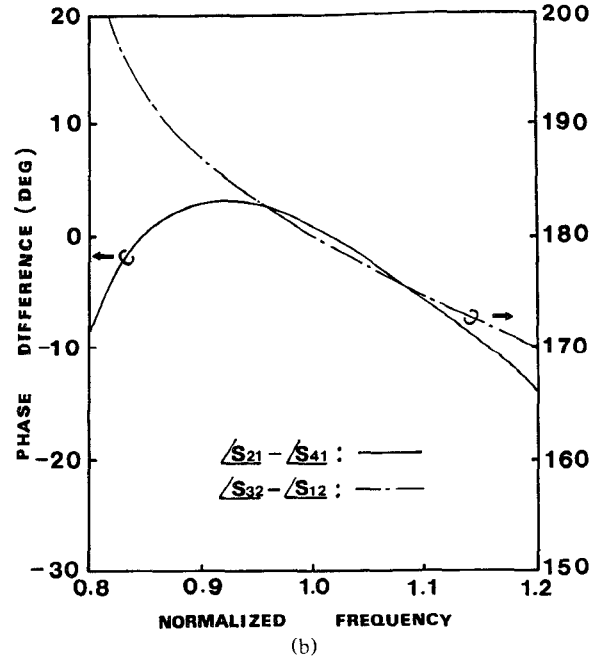

(b)

Fig. 6. (a)Response curves for the 7/6 wavelength hybrid ring (coupling, isolation, and reflection). (b) Phase differences between outputs of the 7/6 wavelength hybrid ring.

TABLE III
VALUES FOR FABRICATION OF THE DESIGNED 3 dB HYBRID-RING DIRECTIONAL COUPLER USED IN EXPERIMENTS

Sections	Normalized Admittance	ϵ_{eff}	λ_g (mm)	Line Width (mm)
$Y_1 = Y_3$	0.577	2.026	22.422	0.625
Y_2	0.816	2.103	22.008	1.202

The relative dielectric constant $\epsilon_r = 2.60$; thickness of substrate $h = 0.6$ mm; design center frequency $f_0 = 9.4$ GHz; loss tangent $\tan\delta = 0.0022$.

TABLE IV
VALUES FOR FABRICATION OF THE DESIGNED 3 dB HYBRID-RING DIRECTIONAL COUPLER USED IN EXPERIMENTS

Sections	Normalized Admittance	ϵ_{eff}	λ_g (mm)	Line Width (mm)
$Y_1 = Y_2 = Y_3$	0.866	2.116	21.94	1.327

The relative dielectric constant, etc., are the same as in Table III.

tional coupler designed in Section II, while Fig.6(b) shows the phase differences between outputs for the coupler. The characteristic admittance and the length of each section are represented in Table II.

IV. EXPERIMENTAL RESULTS

To confirm the validity of the proposed design method of the new 3 dB hybrid-ring directional couplers, we have fabricated the circuits on microstrip line and tested their frequency characteristics. The effective dielectric constant, the wavelength, the linewidth, and the line impedance in the microstrip have been calculated in [8] and [9]. The calculated values for constructing the proposed new 3 dB hybrid-rings at a center frequency of 9.4 GHz are given in Tables III and IV.

Figs. 7 and 8 show the circuits fabricated for the experiments, one the 1.25λ-ring and the other the 7λ/6-ring directional coupler. Because of variations in the effective dielectric constant in microstrip, the lengths of the sections on the ring circumference should be different. However, for purposes of convenience, in the experiments we constructed the networks by using the mean value of the wavelengths on the circumference, i.e., neglecting differences of the wavelengths caused by differences of the line impedanees.

Figs. 9 and 10 show the measured frequency characteristics obtained from the experiments for the proposed 3 dB directional couplers with 1.25λ-ring and 7λ/6-ring circumferences constructed as described above, while the theoretical responses are shown in Figs. 5(a) and 6(a), respectively. The frequency

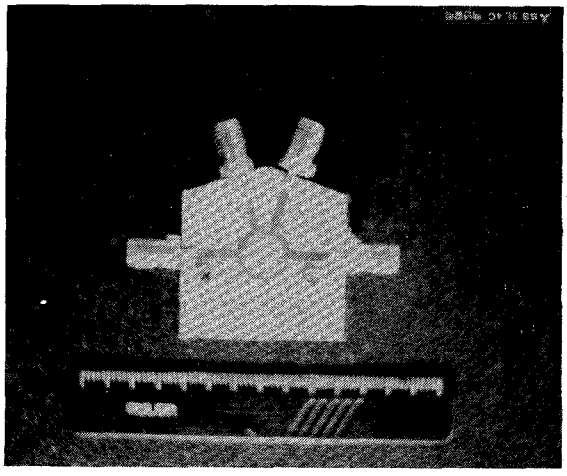

Fig. 7. Photograph of the fabricated 1.25λ-ring directional coupler.

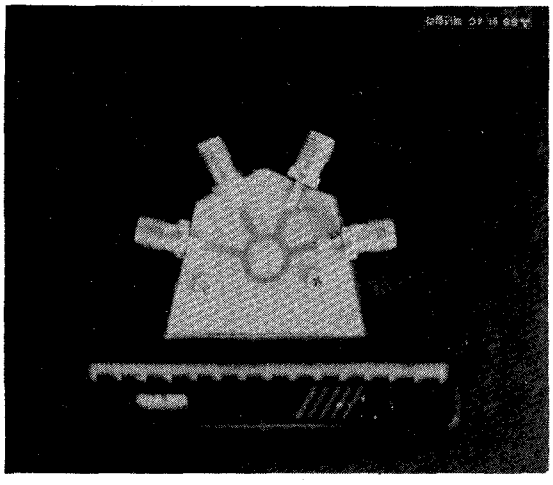

Fig. 8. Photograph of the fabricated 7λ/6-ring directional coupler.

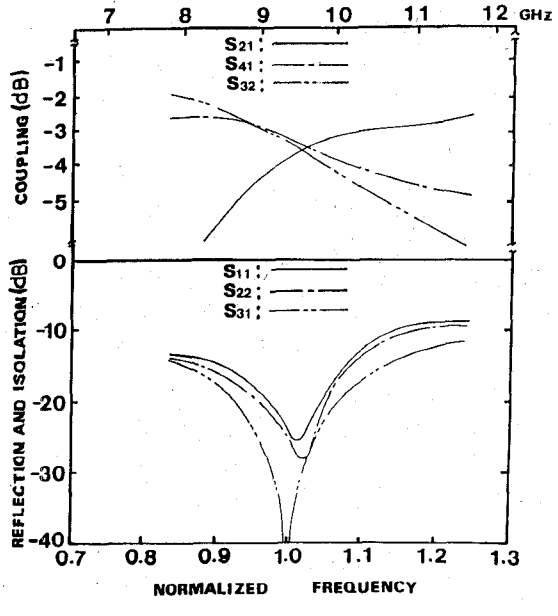

Fig. 9. Measured response curves for the 1.25λ-ring directional coupler.

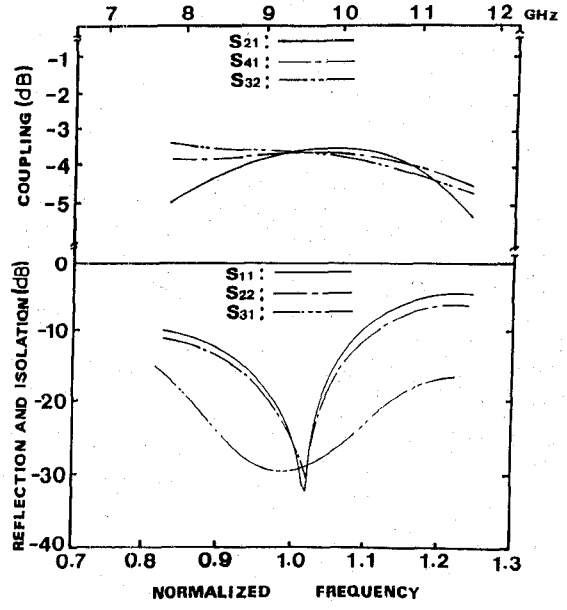

Fig. 10. Measured response curves for the 7λ/6-ring directional coupler.

characteristics agree reasonably well with the designed ones in spite of neglecting the wavelength differences in the ring sections.

On the other hand, the levels of equal splits were about 3.3 dB, owing to loss, this is a marked improvement over [5] in spite of the high frequency band. Therefore, the insertion losses are decreased by virtue of the short lengths of the ring circumferences by using λ/8 or λ/6 lines.

V. Conclusion

A new design theory for 3 dB hybrid-ring directional couplers using λ/8 or λ/6 line has been proposed. Moreover, 1.25λ-ring and 7λ/6-ring directional couplers have been designed and analyzed. Furthermore, the experiments for both cases were carried out, the results of which agreed well with the theoretical ones. Hence, the validity of the proposed design method was confirmed.

References

[1] W. V. Tyminski and A. Z. Hylas, "A wide-band hybrid ring for UHF," *Proc. IRE*, vol. 41, pp. 81–87, Jan. 1953.

[2] C. Y. Pon, "Hybrid-ring directional coupler for arbitrary power division," *IRE Trans. Microwave Theory Tech.*, vol. 9, pp. 529–535, Nov. 1961.

[3] M. Arditi, "Characteristics and applications of microstrip for microwave wiring," *IRE Trans. Microwave Theory Tech.*, vol. 3, pp. 31–56, Mar. 1955.

[4] K. Agrawal and G. F. Mikucki, "A printed-circuit hybrid-ring directional coupler for arbitrary power divisions," *IEEE Trans. Microwave Theory Tech.*, vol. MTT-34, pp. 1401–1407, Dec. 1986.

[5] D. I. Kim and Y. Naito, "Broad-band design of the improved hybrid-ring 3 dB directional coupler," *IEEE Trans. Microwave Theory Tech.*, vol. MTT-30, pp. 2040–2046, Nov. 1982.

[6] W. A. Tyrrell, "Hybrid circuits for microwaves," *Proc. IRE*, vol. 35, pp. 1294–1306, Nov. 1947.

[7] J. Reed and G. J. Wheeler, "A method of analysis of symmetrical four-port network, *IRE Trans. Microwave Theory Tech.*, vol. 4, pp. 246–252, Oct. 1956.

[8] M. V. Schneider, "Microstrip line for microwave integrated circuits," *Bell Syst. Tech. J.*, pp. 1421–1445, May–June 1969.
[9] V. F. Fusco, *Microwave Circuit Analysis and Computer Aided Design*. Englewood Cliffs, NJ: Prentice-Hall, 1987.

A Comparison of Two Approximations for the Capacitance of a Circle Concentric with a Cross

Henry J. Riblet

Abstract—**The maximum and minimum capacitances on circles concentric with an internal cross are determined for a four-lobed as well as an eight-lobed equipotential distribution. The average and geometric mean of these extreme capacitances are then compared with the exact capacitance. The increased accuracy obtained from the eight-lobed equipotential distribution is presented in graphical form.**

I. Introduction

Oberhettinger and Magnus [1, p. 44] showed how the interior of a regular polygon can be mapped into the interior of a circle, and later Laura and Luisoni [2] showed how the exterior of a regular polygon can be mapped onto the exterior of a circle. In the latter case, circles exterior to the circle can be mapped back onto equilobed curves exterior to the polygon. Laura and Luisoni obtained power series for these transformations and showed that these equilobed curves approach circles as they become increasingly distant from the inner polygon. In this short paper, for the special case considered, it will be shown how equilobed curves of this type can be replaced by circles with only a small change in capacitance.

The case in which the inner polygon is a cross is of interest in this connection. In the first place, the exact solution to the problem of determining the capacitance of a cross in a circle is known [3, p. 1821] so that the accuracy of any approximate solution is available. Moreover, it will be shown that the method used in [1] and [2], when applied to mapping the exterior of a circle onto the exterior of cross, results in an integral which can be evaluated in closed form. This makes it a simple matter to determine the four-lobed curves bounding the region about the cross into which the area between the concentric circles is mapped. Another approximate solution to this problem is provided by the known mapping of the region between a cross and a square onto a rectangle [4]. In this case the equilobed curve surrounding the cross is eight-lobed. This short paper compares the accuracy of the four-lobed approximation with that of the eight-lobed approximation. In the first place, it is found that the relative difference between the maximum and minimum "effective" capacitances of the eight-lobed curves is about an order of magnitude lower than the same difference in the four-lobed curves, for comparable geometries. Moreover, it is shown that the average and the geometric means of the maximum and minimum "effective" capacitances on the multilobed curves are excellent approximations to the exact values. In fact, the error in the average of the maximum and minimum "effective" capacitances decreases exponentially as their relative difference decreases so that the average value for the eight-lobed case is a better approximation than the average for the four-lobed case by at least an order of magnitude, in the cases of most interest.

Manuscript received November 5, 1990; revised May 29, 1991.
The author is with Microwave Development Laboratories, Inc., 10 Michigan Drive, Natick, MA 01760.
IEEE Log Number 9102325.

II. The Exact Solution

Fig. 1 shows the successive mapping of a quadrant of a circle onto the upper half plane. The transformation

$$t = -\frac{1}{2}\left(z + \frac{1}{z}\right) \tag{1}$$

maps the upper right-hand quadrant of the circle onto the upper half plane so that two arms of the cross fall on the real and imaginary axes as shown in Fig. 1. Then the further transformation

$$w = t^2 \tag{2}$$

maps the upper right-hand quadrant of the t plane onto the upper half of the w plane. The capacitance, C, in the upper half w plane, between the line segment, fa, and the infinite line segment, bg, is given by the well-known formula [5, p. 58]

$$C = \frac{K(k)}{K'(k)} \tag{3}$$

where, in our case,

$$k^2 = \frac{(a-f)(g-b)}{(g-a)(b-f)} \tag{4}$$

$$= \frac{8\delta^2(1+\delta^4)}{(1+\delta^2)^4}. \tag{5}$$

The total capacitance, C_0, of the cross in the circle is then given by

$$C_0 = 4\frac{K(k)}{K'(k)} \tag{6}$$

where k is given by (5) and δ is the ratio of the length of the arms of the cross to the radius of the circle.

The AGM series [6, p. 331], where the convergence is very rapid, was used to calculate K and K', given k. It is values obtained in this way that are considered in this paper to be exact.

III. The Four-Lobed Case

The problem of mapping the exterior of a circle onto the exterior of a cross is solved by combining the ideas of Laura and Luisoni [2] with those of Oberhettinger and Magnus [1, p. 42]. It is found that the required transformation is given by the integral

$$w = \frac{1}{2}\int_0^z \frac{z^4-1}{z^2\sqrt{z^4+1}}\,dz. \tag{7}$$

In turn, this can be integrated in closed form to give

$$w = \frac{\sqrt{z^4+1}}{2z}. \tag{8}$$

That this function maps the unit circle in the z plane of Fig. 2 onto the unit cross in the w plane is readily seen by replacing z